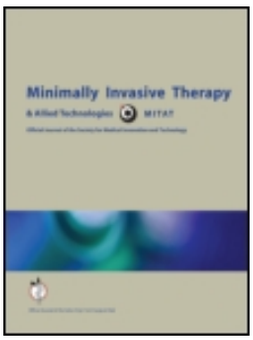

Minimally Invasive Therapy & Allied Technologies

ISSN: 1364-5706 (Print) 1365-2931 (Online) Journal homepage: https://www.tandfonline.com/loi/imit20

Control of soft tissue deformation during robotic needle insertion

Niki Abolhassani, Rajni Patel & Mehrdad Moallem

To cite this article: Niki Abolhassani, Rajni Patel & Mehrdad Moallem (2006) Control of soft tissue deformation during robotic needle insertion, Minimally Invasive Therapy & Allied Technologies, 15:3, 165-176, DOI: 10.1080/13645700600771645

To link to this article: https://doi.org/10.1080/13645700600771645

Minimally Invasive Therapy. 2006; 15:3; 165–176

Taylor & Francis
Taylor & Francis Group

ORIGINAL ARTICLE

Control of soft tissue deformation during robotic needle insertion

NIKI ABOLHASSANI, RAJNI PATEL & MEHRDAD MOALLEM

Department of Electrical and Computer Engineering, University of Western Ontario, London, Canada

Abstract
Accurate needle insertion into soft, inhomogeneous tissue is of practical interest because of its importance in percutaneous therapies. In procedures that involve multiple needle insertions such as transrectal ultrasound-guided prostate brachytherapy, it is important to reduce tissue deformation before puncture and during needle insertion. In order to reduce this deformation, we have studied the effect of different trajectories for a 2-DOF (degrees of freedom) robot performing needle insertion in soft tissue. To obtain an optimum trajectory, we have compared tissue indentation and frictional forces for different trajectories. According to the results of our experiments, infinitesimal force per tissue displacement is a useful parameter for online trajectory update. In addition, the results show that axial rotation can reduce tissue indentation before puncture and frictional forces after puncture. Our proposed position/force controller is shown to provide considerable improvement in performance with regard to minimizing tissue deformation before puncture.

Key words: *Needle insertion, needle rotation, insertion forces, prostate brachytherapy, tissue deformation*

Introduction

There has been very significant interest in the application of robotics in surgery and therapy in recent years. The use of robots may provide enhanced accuracy, minimum invasiveness, and in some cases reduced operation times. In many of the computer-assisted procedures, a robot is used to locate a position and insert a needle or a catheter quickly and accurately (1,2). In computer-assisted procedures where the position is a fixed target such as in orthopedic surgery (3), preinterventional/presurgical paths provide satisfactory accuracy since there is no significant target displacement during insertion (1). In recent studies the main focus has been on the insertion of a needle or a catheter into soft tissue or organs. The complication of these procedures is due to tissue deformation and organ movement during insertion, which cause displacement of the target. Tissue deformation is due to the mechanical properties of soft tissue, needle tip contact force, and frictional forces between the tissue and the needle shaft (2,4–6), and reduces the effectiveness of the therapy (7).

Prostate brachytherapy is an example of a procedure involving needle insertion into soft tissue. The prostate brachytherapy technique involves the permanent implantation of radioactive pellets (e.g. ^{125}I or ^{103}Pd) within the prostate. Figure 1 shows the current manual procedure for prostate brachytherapy (8). First, the transrectal ultrasound (TRUS) probe is inserted into the rectum and when the surgeon is satisfied with the imaging, the probe is locked in position. The therapy requires multiple needle insertions using a template grid for needle guidance while imaging of the prostate area is carried out using TRUS. Needle insertion can be divided into two parts in this procedure. The first part starts when the needle is still outside the patient's body and continues until the needle is in the neighborhood of the prostate, i.e. until the needle tip reaches the ultrasound field of view. From that point onwards, the second part of the needle insertion procedure begins. It ends when the needle tip reaches the target. Needle insertion in the second part can benefit from visual feedback while in the first part, only kinesthetic feedback from the tool exists. It is well known that less tissue deformation (movement) before puncture and during needle insertion results in less movement of the prostate and therefore requires less needle steering and less

Correspondence: N. Abolhassani, Department of Electrical and Computer Engineering, University of Western Ontario, 1151 Richmond Street North, London, Ontario, Canada N6A 5B9. Fax: +1-519-663-8401. E-mail: nabolhas@uwo.ca

ISSN 1364-5706 print/ISSN 1365-2931 online
DOI: 10.1080/13645700600771645

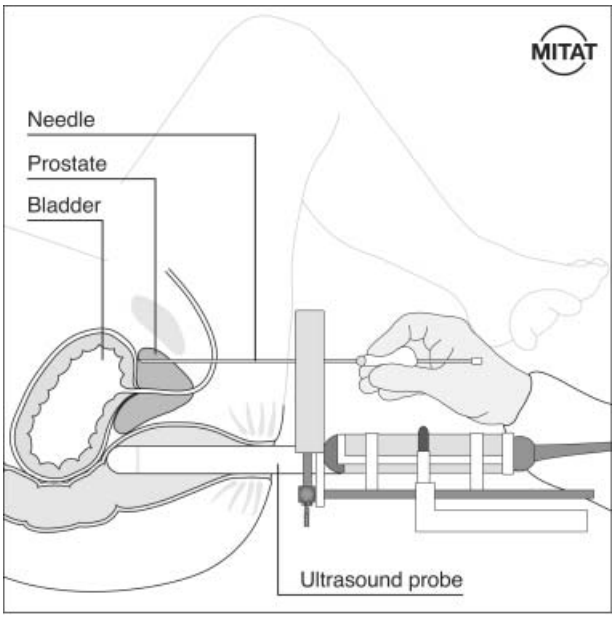

Figure 1. Prior to needle insertion, the ultrasound probe is inserted into the rectum and locked in position (8).

frequent re-setting of the TRUS probe to provide good imaging of the area.

Transperineal needle insertion for prostate biopsy is another example of percutaneous procedures which would benefit from less tissue deformation while the needle is being guided to the target location. In biopsies, when the needle tip is not located with sufficient accuracy, more needle steering is required. In such procedures, it is desirable to insert the needle with minimum steering and less damage to surrounding tissue.

The goal of the research described in this paper was to investigate and analyze the effect of different motions on needle insertion in soft, inhomogeneous tissue, and eventually to generate trajectories for needle insertion that result in less tissue deformation during insertion and before puncture. In this study, we use the expression ''tissue indentation'' to refer to tissue deformation before puncture.

This paper is organized as follows. First, related work in the areas of tissue deformation and modeling, needle insertion force modeling, and force measurement in automated insertions is discussed. Second, the experimental methods are explained. Third, the results for each set of experiments are presented. Fourth, the results are compared in order to find a suitable trajectory for computer-assisted needle insertion.

Related work

In percutaneous therapies, the needle punctures and passes through different tissue layers such as skin, muscle, fatty and connective tissue. Puncturing and cutting each of these layers require different amounts of force. The amount of force even varies from patient to patient for the same tissue type. Also, due to the difference in mechanical properties, each tissue type deforms differently during needle insertion. Recent studies have focused on improving the precision of the percutaneous procedures from several different aspects. The main categories are briefly reviewed here:

Modeling interactive forces during needle insertion

All recent studies show that the axial force of a needle during insertion in soft tissue is the summation of different forces distributed along the needle shaft (2,5,9). Using a specially developed 7-axis load cell for measuring and separating forces during needle insertion, Kataoka et al. (5) performed experiments on a canine prostate. Three different forces acting on the needle were measured independently: The tip force, the friction force, and the clamping force. The tip force decreases immediately after puncture to the value for the cutting force. The other two forces increase as the needle is inserted into tissue. DiMaio and Salcudean (2,10) explored the relationship between needle force and 2D tissue deformation. They presented a force distribution along the needle shaft. This distribution indicates the existence of two forces: An axial friction between the needle and the tissue, which is uniform along the shaft, and a force peak at the needle tip, which results from tissue cutting and rises approximately 30% above the friction force (10).

Okamura et al. (9) investigated modeling of needle insertion forces for bovine liver and considered puncture of the capsule as an event which divides the insertion into pre-puncture and post-puncture phases. The capsule stiffness is a pre-puncture force and increases steadily until a sharp drop in the amount of force identifies the puncture event. During post-puncture, the amount of force is variable due to friction, cutting, and collision with interior structures. They modeled the stiffness force by a nonlinear spring model, friction by a modified Karnopp model (11), and cutting forces as the remaining forces which are constant for a given tissue. Maurin et al. applied two models to the data obtained from needle insertion into liver and kidney of anesthetized pigs (12). The first model was taken from Okamura et al. (9). They fitted a second order polynomial to the data for modeling the stiffness force and the Karnopp model for the friction force. The second model was taken from Maurel (13) and based on the work of Fung (14). Their modeling showed low errors for both models.

Force data in some procedures are used for identifying the tissue layer as the needle is inserted. Brett et al. studied the effect of force sensory data for stapedotomy (15) and epidural puncture (16). Matsumiya et al. presented an experimental study of robotic needle insertion into human vertebra and measured forces and torques during insertion (17). The results show a strong correlation between the axial force variation during insertion and the distribution of the bone local CT-value along the needle path. It was shown that forces during robotic insertion into human femoral head are much smaller than those during manual insertion.

Modeling and simulation of tissue deformation

According to Cotin, for modeling soft tissue it is necessary to determine the biomechanical properties through *in vitro* and *in vivo* measurements, to use constitutive laws and develop spring-mass or finite element models (FEM) for real-time simulations (18). There are many articles on the mechanical properties of biological tissue systems and *in vitro* measurement of soft tissues (14,19,20). Recently researchers have been exploring different methods to obtain quantitative information on the biomechanical properties of *in vivo* soft tissue. Han et al. (21) introduced a prototype ultrasound indentation system to compare various methods for measuring *in vivo* biomechanical properties. Menciassi et al. (22) presented a smart robotic micro-instrument for measuring *in vivo* tissue properties, both qualitatively and quantitatively. Ottensmeyer et al. (23) performed four categories of experiments for measuring viscoelastic properties of soft tissue: *in vivo*, *in vitro* excised lobe case, *ex vivo* whole organ with perfusion and *ex vivo* whole organ without perfusion. They used the TeMPeST (Tissue Measurement Property Sampling Tools) instrument (24) for measuring the compliance of solid organ tissues *in vivo*. They also built an apparatus to maintain cellular integrity during *ex vivo* experiments. They found that testing the whole organ provides a more accurate reference than a cut specimen. Also, in their experiments with the perfusion apparatus, the large deformation time responses approached those of tissues tested *in vivo*. Other work for *in vivo* measurement of soft tissue is described in ref. 25–28.

DiMaio and Salcudean (2,6) have performed extensive studies on simulation of tissue deformations that occur during needle insertion in soft tissue. They achieved real-time modeling of needle insertion in soft tissue using FEM. Alterovitz et al. (4,29) have presented FEM modeling and simulation of needle insertion with application to prostate brachytherapy. Tissue deformations during the needle insertion and retraction phases, which lead to imprecise seed placement, were considered in their simulation studies. Alterovitz et al. (4) described the sensitivity of the seed placement error to changes in physician-controlled parameters such as depth and height of needle insertion, needle sharpness, friction, velocity of needle insertion as well as patient-specific parameters such as Young's Modulus and tissue stiffness. Their analysis suggests that reducing friction and tissue deformation can decrease seed placement error.

Kerdok et al. (30) investigated the deformation of a cube of soft polymer (silicon) that is referred to as the ''truth cube''. They placed beads in a grid pattern throughout the volume of the cube. The displacement of the beads was measured using CT-scan images when the cube was under pressure. Boundary conditions, material properties and bead displacement were used to compare the performance of real-time modeling of deformation using FEM. Their work studied the tradeoff between the accuracy of FEM versus its computational cost. As the next step in this study, Howe (31) replaced the truth cube by a whole real organ (liver) that was perfused with physiological solutions at pressures and temperatures mimicking *in vivo* circulatory conditions. The relaxation modulus and creep modulus were measured and constitutive law parameters that result in an accurate FEM were calculated. They showed that their setup maintained *in vivo* mechanical responses of the liver.

Modeling needle deflection during insertion

The thin needle has to pass through many different tissue layers of varying resilience, which makes the net deflection difficult to predict. Kataoka et al. (32) used a physical quantity called infinitesimal force per unit length in order to find the relation between tissue deformation and needle deflection. In their model, this quantity is adopted instead of traction because of the long thin shape of the needle. Okamura et al. (9) investigated the effect of needle geometry on insertion forces and needle bending. They found that the tip type has a significant effect on insertion forces. Moreover, bevel tip needles lead to more needle bending. From their results, increasing needle diameter generally increases the insertion forces but reduces needle bending. Webster et al. (33) performed needle insertion into a rubber-like simulated muscle. They used needles with different bevel angles. Their results show that decreasing the bevel angle increases the amount of needle deflection (bending), and the bevel angle has little impact on

the amount of axial force. They also found that the velocity of needle insertion in homogeneous, relatively stiff phantom tissue had no discernible effect on the amount of needle deflection.

Needle guidance and steering

DiMaio and Salcudean (2) used their needle insertion model (FEM) to study the motion-planning problem and introduced a ''needle manipulation Jacobian'' for needle steering and manipulation. Similar to the steering technique of DiMaio and Salcudean but with a simplified model for the tissue and flexible needle, Glozman and Shoham (34) were able to do fast path planning and real-time tracking for the needle in order to avoid an obstacle and hit a target. To simplify the model, they approximated the tissue using springs and employed an inverse kinematics approach to translate and orient the needle base. They found that the needle base trajectory can be varied and can be optimized to minimize lateral pressure of the needle shaft on the tissue. Webster et al. developed a ''bicycle-like'' nonholonomic[1] model for steering flexible bevel-tip needles in rigid tissues (35). Unlike the approach presented by DiMaio and Salcudean, their needle is flexible relative to the tissue and needle steering does not displace a large amount of tissue. Their experiments showed that the needle tip followed a circular arc that also fits the curvature obtained from the proposed model. Actual control and steering was not done in their experiments.

While other researchers have investigated different models for needle steering and a few models for simulation of a needle insertion procedure, control of a needle during insertion from the perspective of less tissue deformation (without the availability of a deformation model), as reported in this paper, has not been done. This paper compares the effect of different computer-generated needle motions on tissue indentation and frictional forces. Changes in frictional forces affect the amount of tissue deformation during needle penetration (4).

Experimental setup

A test-bed has been set up in our laboratory for studying needle insertion in soft tissue. This provides needle motion with two degrees of freedom (DOF) — translation in one (horizontal) direction and rotation about the translational axis. The needle insertion is performed using the translational motion. The axial rotation is added to study its effect on friction and tissue deformation while the needle is being inserted into soft tissue. As in the actual procedure, the needle holder is capable of holding a needle such that there is a space of about 7 cm from the tip of the needle for radioactive seeds. A 6-DOF force/torque sensor is attached to the needle holder to measure the forces and torques acting on the needle. The 6-DOF force/torque sensor is a Nano43 DAQ F/T system from ATI Industrial Automation Apex, NC, USA). In the experiments, an 18-gauge needle with a beveled tip (22° bevel angle) was used which is the typical medical needle used for the prostate brachytherapy procedure. The needle can flex quite easily. Therefore it cannot be assumed to be perfectly straight at insertion time.

A multi-threaded application for position/velocity control, force reading and data acquisition has been developed using Microsoft® Visual C++. This application runs on a Pentium 4, 2.4 GHz computer, with Microsoft® Windows 2000 as its operating system. The application is written such that the force readings are obtained at the rate of 1 kHz, the control thread uses a servo rate of 25 Hz, and the graphical user interface (GUI) is updated at the rate of 8 Hz. High frequency force readings are required to capture sudden changes in the forces at different stages of needle insertion. The application has a GUI which enables the user to define the speed and depth of insertion as well as the speed and direction of the needle rotation. Motions with constant and variable velocity can be defined and force/torque readings can be displayed. A proportional-integral-derivative (PID) control scheme is used to control the needle motion in order to track specified trajectories in both degrees of freedom during needle insertion.

Experiments were carried out on two-layer phantoms of turkey tissue with their skin intact. Although the characteristics of this tissue are not similar to those of the prostate, it was chosen because of its inhomogenous, nonlinear and visco-elastic properties which made it better suited for the experiments than artificial phantoms such as silicone-based materials. It was found that artificial phantoms which were thin and nonlinearly inhomogeneous were difficult to construct. Also artificial multi-layer phantoms are difficult to make as there is no single material that can satisfy the properties required for different layers. Furthermore, gluing different materials together or placing them next to each other without gluing them together (sandwich phantoms) could give misleading results for needle insertion. To

[1]The term nonholonomic refers to systems that have interdependent constraints on the kinematic model. These constraints are in differential form and are not integrable.

the best of our knowledge, there is no phantom on the market that can overcome the problems mentioned above, which can be used as a reference for the prostate with all its inherent mechanical properties. There are a few training phantoms which are only accurate in terms of optical properties; however, the mechanical properties of these are not specified. It should be emphasized that the goal of this work was to work with multi-layered phantoms with inhomogeneous nonlinear visco-elastic properties and to find a trajectory that is suitable for guiding the needle from a point on the surface to a point inside the phantom. Numerically different results might be observed for *in vivo* experiments due to differences in the elasticity of the tissue, moisture and blood circulation. However the approach developed in this paper provides an indication of the behavior of needle insertion in nonlinear visco-elastic inhomogeneous animal tissue. The test-bed for the experiments is shown in Figure 2.

Methods

This work resulted from a project involving needle insertion in TRUS-guided prostate brachytherapy. In the TRUS-guided prostate brachytherapy procedure, about 20 needles are inserted (Figure 1) with each needle containing about five seeds. The length of each seed is about 4 mm and its thickness is <1 mm. As is well known, the effectiveness of the treatment depends on the accuracy with which the radioactive seeds can be placed. The TRUS probe requires re-setting for any tissue movement in order to provide good imaging of the prostate area. Moreover, in this procedure, the needle has to pass through 7–10 cm of skin, muscle and fatty tissue before it reaches the prostate, i.e. before it is detectable by the TRUS imaging system. This means that reducing tissue deformation and limiting the movement of the target organ behind the tissue is important. Therefore, our experiments were conducted with the goal of developing an approach for needle insertion that reduces tissue indentation (deformation before puncture) and frictional forces. Reducing frictional forces indirectly reduces tissue deformation during needle insertion and retraction procedures (4,29).

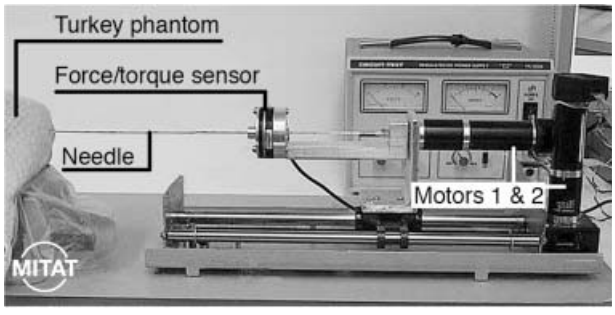

Figure 2. The experimental setup.

In our experiments, the needle is moved toward the tissue until the force sensor gives a non-zero force reading in the Z (insertion) direction. This denotes the point where the needle touches the tissue. Then a desired trajectory is generated and the needle motion is controlled to track the trajectory. The depth of insertion is set to 4 cm beyond the skin contact point. The insertion continues until a sharp drop in the amount of force in the Z (insertion) direction is detected by the sensor. This is the point where the needle punctures the tissue. The skin contact point and the tissue puncture point are used to calculate tissue indentation for each insertion.

Needle insertion trajectories consist of different types of translational and rotational motions. The experiments were divided into four groups based on the method used for needle insertion and the parameter which was measured (Table I).

Group one compared the effect of different translational trajectories for the needle motion. The difference in trajectories for group one was related to the variation of velocities and accelerations. The accelerated motion was tried because from clinical procedures it was found that the surgeon exerts more force in short periods on the needle in order to puncture the tissue.

In Group two and Group three, for each constant velocity along the translational axis, the effects of different rotational motions of the needle were compared. The following were considered: No rotation, continuous rotation with different speeds, partial rotation in two alternating directions with different speeds and degrees, and needle rotation based on the value of forces in the X–Y plane (Z-axis being the insertion direction). However in Group two experiments, the measured quantity was tissue indentation and in Group three experiments it was frictional force. In Group three, the experiments made use of a cubic container with a hole in the center (Figure 3). The tissue phantom was placed in the container filling the entire volume of the container. This setup constrained tissue displacement and maintained a constant thickness of tissue for each test (9). To ensure that the force measurements were not affected by this constraint, several preliminary insertions with different translational velocities without any constraint were performed, and the results were found to be comparable.

Table I. Summary of the experimental groups.

Group Number	Translational Motion	Rotational Motion	Measured Parameter
1	Constant velocity Constant acceleration Variable acceleration	None	Indentation
2	Constant velocity (10mm/s)	a. None b. Continuous rotation c. Bi-directional rotation (different angles) d. Rotation control using X and Y forces	Indentation
3	Constant velocity (10mm/s)	a. None b. Continuous rotation) c. Bi-directional rotation (different angles d. Rotation control using X and Y forces	Friction
4	Online update of velocity	a. None b. Rotation control using X and Y forces	Indentation

In Group four experiments, we used the quantity $K_e = \lim_{\Delta x \to 0} (\Delta f / \Delta x)$, the infinitesimal tissue force per tissue displacement in the insertion direction before puncture. In a simple mass-spring model of tissue, K_e is actually considered to be tissue stiffness. In a polynomial stiffness model of skin tissue, this quantity is not constant (32). It reaches its maximum at the point of puncture. This physical quantity was used to update the trajectory during insertion.

In the experiments, each insertion was done at a different location of the phantom in order to avoid the artifact caused by the holes created during previous insertions. However, each set of insertions was made in a close neighborhood to have consistent tissue behavior for the set. During the experiments, we noted that the orientation of the beveled edge of the needle has an effect on the amount of bending in the needle. Therefore, for consistency, we did all our experiments with the same upward orientation of the needle bevel at the skin contact point. For each experiment, the validity of needle motion was verified by plotting the data for the needle position, velocity and acceleration using MATLAB.

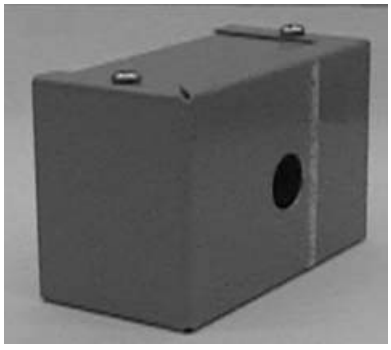

Figure 3. The cubic container with a hole in the center on both sides for needle insertion.

Results

It is important to note that each group of experiments was performed at different times with different turkey tissues. Therefore the results of each group should only be compared with the results within that group. The purpose of these experiments was not to build a database. The purpose was to find how different insertion techniques could reduce tissue deformation. In all insertions, Z axis is the insertion direction and X and Y axes are in the plane orthogonal to the insertion direction.

Group 1 experiments

These experiments compared the effect of different velocities and accelerations for translational motion on tissue indentation.

- *Trajectories with constant velocity*: Trajectories with constant velocity for translational motion with no rotational motion were generated. Translational velocities varied from 1 mm/s to 20 mm/s. This is the possible range for manual needle insertion based on the feedback of the physicians. The needle insertion data was logged for 25 insertions. The results showed that increasing velocity reduces tissue indentation up to a certain point. There was not a consistent improvement and dramatic difference in the amount of tissue indentation for high translational velocities. Table II summarizes the results of tissue indentation for needle insertions with different translational velocities. We considered a translational velocity of 10 mm/s without rotation as the standard for comparing with other types of trajectories. The average indentation for insertion with a velocity of 10 mm/s was 12.4 mm.
- *Trajectories with constant acceleration*: In these experiments, trajectories with constant acceleration for translational motion with no rotational

Table II.The effect of different translational velocities on tissue indentation. All motions are compared to the motion with constant velocity of 10 mm/s.

Velocity (mm/s)	Average tissue indentation (%)
1	127
5	107
10	100
15	105
20	107

motion were generated. We used the following accelerations: 3 mm/s^2, 7 mm/s^2, and 10 mm/s^2. All trajectories had zero initial velocity. The result for this method had no consistency. They also did not show any consistent improvement over the standard trajectories (i.e. constant velocity of 10 mm/s).

- *Trajectories with variable acceleration*: In these experiments, quintic polynomial trajectories for translational motion with no rotational motion were generated (36). The coefficients for the quintic polynomial were set so that the trajectories would not saturate the input voltage and the maximum velocity did not exceed 23 mm/s. The results for this method also had no consistency. They also did not show any consistent improvement over the standard trajectories (i.e. constant velocity of 10 mm/s).

Group 2 experiments

In this group, trajectories with constant velocity for rotational motion were generated while a constant velocity of 10 mm/s for translational motion was maintained. Rotational velocities varied from 1 rpm to 25 rpm. Each set of tests consisted of the following cases:

- No rotational motion
- Continuous rotational motion in one direction, e.g. rotating the needle with a speed of 3 rpm clockwise
- 90° rotational motion in each direction about its nominal (zero) position
- 30° rotational motion in each direction about its nominal (zero) position
- 10° rotational motion in each direction about its nominal (zero) position
- Controlling the direction of needle rotation using forces in the X and Y directions, e.g. keeping them as close to zero as possible.

The needle insertion data was logged for 20 insertions for each type of motion. The results for

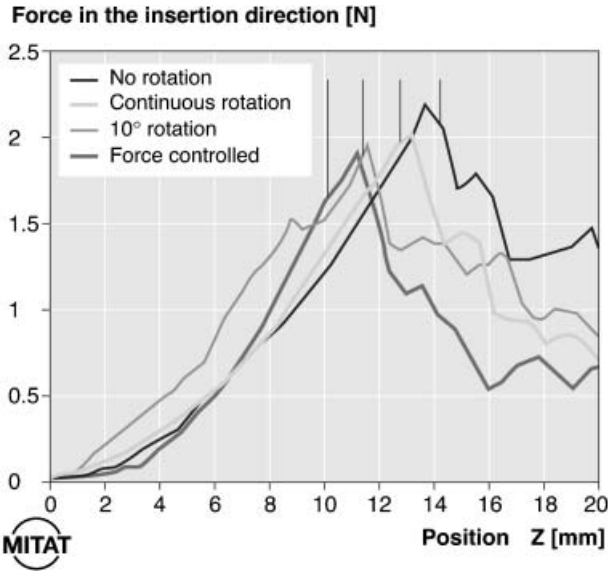

Figure 4. Comparison of the effects of different rotational motions on tissue indentation (The translational velocity for this experiment was set to 10 mm/s and the rotational velocity was set to 3 rpm).

the rotational motions showed that they resulted in less tissue indentation before penetration compared to the motions with no rotation. One set of results is shown in Figure 4. Table III summarizes the results for different types of insertions.

It is clear from the results that having rotational motion for the needle during insertion definitely reduces tissue indentation. It was found that the speed of rotation did not have much effect on these values. The results showed that high-speed rotations such as 15 rpm and higher did not yield any significantly less indentation than 5 rpm. The same was found with velocities below 3 rpm. The best region was found to be between 3 and 7 rpm.

Group 3 experiments

The purpose of this group was to measure frictional forces and to investigate the effect of rotational motion on reducing the amount of friction. These

Table III. The effect of different types of needle rotations on tissue indentation. All motions are compared to the motion with no rotation.

Type of motion	Average tissue indentation (%)
No rotation	100
Continuous rotation	89
90° rotation	84
30° rotation	83
10° rotation	80
Rotation control using forces	81

experiments made use of the cubic container shown in Figure 3. In order to measure frictional forces correctly, the needle was first passed completely through the container hole so that there was a constant amount of tissue in contact with the needle at any given time. Then the needle was moved 4 cm backward and forward four times while 10 mm/s constant velocity was maintained along the translational axis. Each set of tests consisted of the following cases:

- No rotational motion
- Continuous rotational motion in one direction, e.g., rotating the needle with a speed of 3 rpm clockwise
- 90° rotational motion in each direction about its nominal (zero) position
- 30° rotational motion in each direction about its nominal (zero) position;
- 10° rotational motion in each direction about its nominal (zero) position;
- Controlling the direction of needle rotation using forces in the X and Y directions, e.g. keeping them as close to zero as possible.

The needle insertion data were logged for 20 insertions for each type of motion. The forces in the Z (insertion) direction were measured during the needle motion and the average was calculated and used for comparison. One set of results is shown in Figure 5. With this experiment, the amount of force read by the force/torque sensor is only the friction along the needle shaft, because there is no tissue cutting involved. Table IV summarizes the results for different types of insertions and the corresponding frictional forces. As presented in this table, the insertions with rotational motion result in less friction, which indirectly means less tissue deformation.

Group 4 experiments

This group of experiments focused on trajectory update during insertion. The idea for trajectory update resulted from an analysis of the data from the previous groups. It is known that the amount of force being exerted on the needle and the velocity of insertion should have an impact on the amount of tissue indentation. Nevertheless, the results of motions with acceleration were not consistent. Therefore, different parameters were considered and finally, $K_e = \lim_{\Delta x \to 0} (\Delta f / \Delta x)$, the infinitesimal force per tissue displacement in the insertion direction before puncture, was chosen. In order to find the value of K_e during insertion and prior to puncture, several insertions were made. The amount

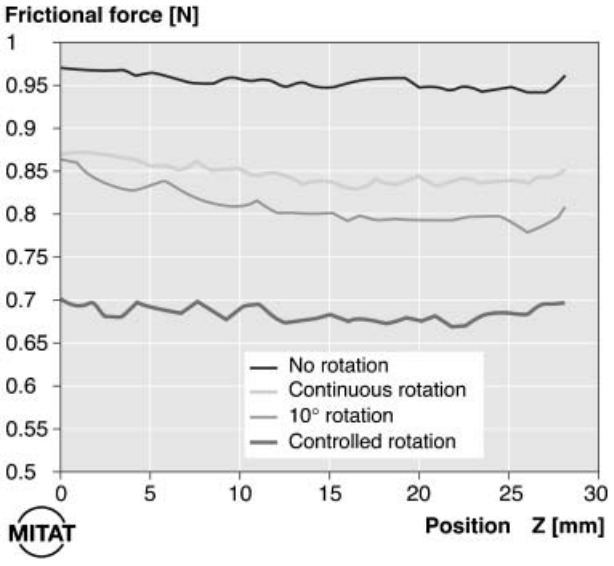

Figure 5. Comparison of the effects of different rotational motions on friction (The translation velocity for this experiment was set to 10 mm/s and the rotation velocity was set to 3 rpm).

of force change and the amount of needle displacement in the insertion direction at each time step were used to calculate K_e. It was noted that in each insertion, K_e increased until it reached the value needed to puncture the skin (Figure 6). The faster that value of K_e was reached during insertion, the less was the tissue indentation. The K_e value is different for different tissue types because of the difference in the mechanical properties of the tissues. The small changes in the value of K_e at the point of puncture in the phantom were due to the inhomogeneity of the tissue layers behind the skin and the skin itself. The average infinitesimal force per tissue displacement at the point of tissue puncture for our phantom was found to be 0.4 N/mm with a standard deviation of 0.13.

In this approach, the average infinitesimal force per tissue displacement at the point of puncture obtained from the first insertion was considered as the desired K_e. Then in subsequent insertions, the velocity of the translational motion was increased in order to achieve the desired K_e faster. To elaborate

Table IV. The effect of different types of motions on frictional force. All motions are compared to the motion with no rotation.

Type of motion	Average frictional force (%)
No rotation	100
Continuous rotation	89
90° rotation	77
30° rotation	85
10° rotation	82
Rotation control using forces	71

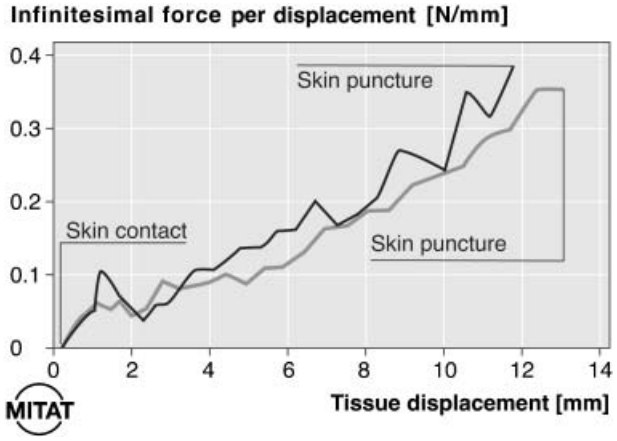

Figure 6. Infinitesimal force per tissue displacement prior to puncture (black line: insertion with constant velocity of 10 mm/s; gray line: insertion with constant velocity of 15 mm/s).

on this approach, the first insertion with the standard trajectory was made in order to calculate the desired value of K_e. From the position/force data logged during this insertion, the desired value of K_e was calculated using

$$K_e = \frac{\sum_{j=i-n+1}^{i} \left(\frac{f_j - f_{j-1}}{x_j - x_{j-1}}\right)}{n} \quad (1)$$

where f_j and x_j are the amount of force in the insertion direction and the tissue indentation respectively at the j^{th} time step, i is the time step of the force peak (tissue puncture), and n is the number of time steps prior to puncture to be used for finding the average value of K_e. Thereafter, in each insertion, initially a trajectory with a constant velocity of 10 mm/s for translational motion was generated. During the insertion in each time step, the controller determined the error between the infinitesimal force per tissue displacement and its desired value. This error was used in a feedback scheme to adjust the velocity of the translational trajectory with a gain factor and to continue to track the new trajectory (Figure 7). Each insertion was continued until a sharp drop was found in the amount of force in the insertion direction. The insertion was then stopped since only the measurement of tissue indentation was required.

Twenty sets of experiments were carried out on turkey phantoms. In each set, one insertion was made with the standard trajectory (i.e. constant velocity of 10 mm/s) and two insertions using the trajectory update method. The results of all the experiments were consistent and showed less tissue indentation for the trajectory update method than

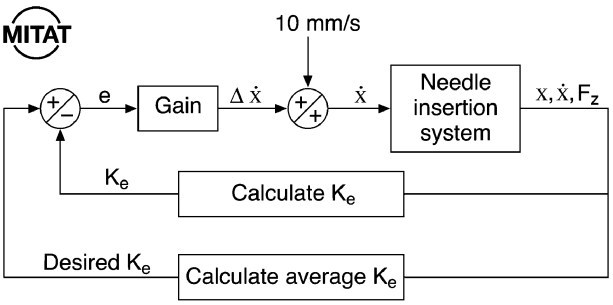

Figure 7. The online update trajectory system. The gain was set to 1.2 mm^2/Ns.

for the standard trajectory. The results of the experiments are summarized in Table V.

From the results of the online trajectory update method, it was found that a linear increase in the velocity of translational motion occurs after the initial velocity of 10 mm/s is reached (Figure 8). This increase in velocity during insertion represents acceleration in the motion due to an additional force exerted at the needle tip during insertion. However, for safety reasons, it is desirable to limit the magnitudes of the velocity so that in case of an emergency, the insertion can be stopped with minimum movement.

Discussion

In order to ensure that the rotation of the needle about the insertion direction (Z-axis) does not cause any problems, the magnitudes of forces in the X–Y plane were investigated. The results are shown in Figure 9. There was a noticeable increase in the magnitudes of forces in the X and Y directions when continuous rotational motion was tried. This increase caused more tissue damage and deformation as a result of defects in the shape of the needle, i.e. as a result of the needle not being perfectly straight. Also, continuous rotation could cause damage by hooking the tissue.

So far we had concluded that incorporation of rotational motion into the insertion would result in less tissue indentation and less frictional force (Tables III and IV). With the results shown in Figure 9, we concluded that control of rotation using forces in X and Y directions has an advantage

Table V. Online update vs. the standard trajectory.

Trajectory Type	Average tissue indentation (%)
Standard (constant velocity of 10 mm/s)	100
Online update	86

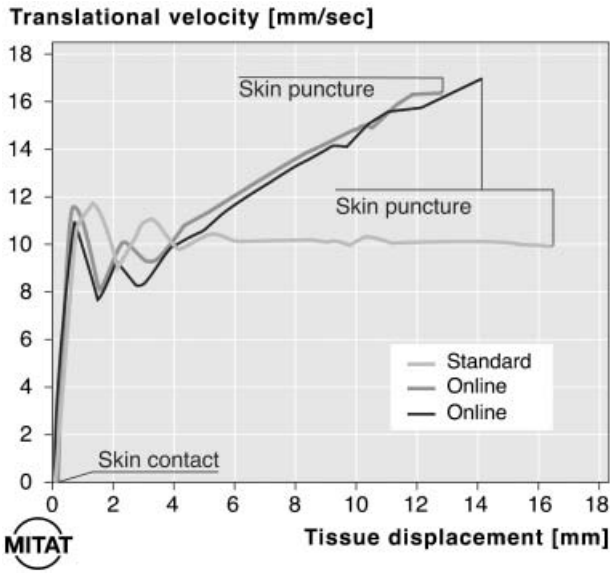

Figure 8. Translational velocity in the standard trajectory and the online trajectory update method.

of causing smaller forces in the X–Y plane, in comparison with rotation without control. Smaller forces in the X and Y directions imply less deformation (movement) of the surrounding tissue as the needle penetrates the tissue. Our ongoing work is concerned with the effect of forces in the X and Y directions on needle deflection.

Also in all insertions, it was realized that after puncture the tissue slides back on the needle and changes the net amount of deformation. To calculate the net deformation, an imaging system is required during insertion. This is part of our ongoing work.

Conclusion

This research was carried out to develop a scheme for trajectory generation for needle insertion in soft tissue, specifically for procedures that require several insertions and initial setup of the imaging system. Different types of needle motion and their effect on tissue indentation prior to puncture and frictional forces during needle insertion were investigated. Tissue indentation, forces and torques during needle insertion in turkey tissue were measured. The insertion forces did not exceed 3.5 N in all cases. It was found that increasing the velocity of translational motion up to a certain point as well as having rotational motion during insertion reduces the amount of indentation. Moreover rotational motion reduces frictional forces. Nevertheless, high velocities should not be selected for safety reasons. Among different rotational motions, it was found that the

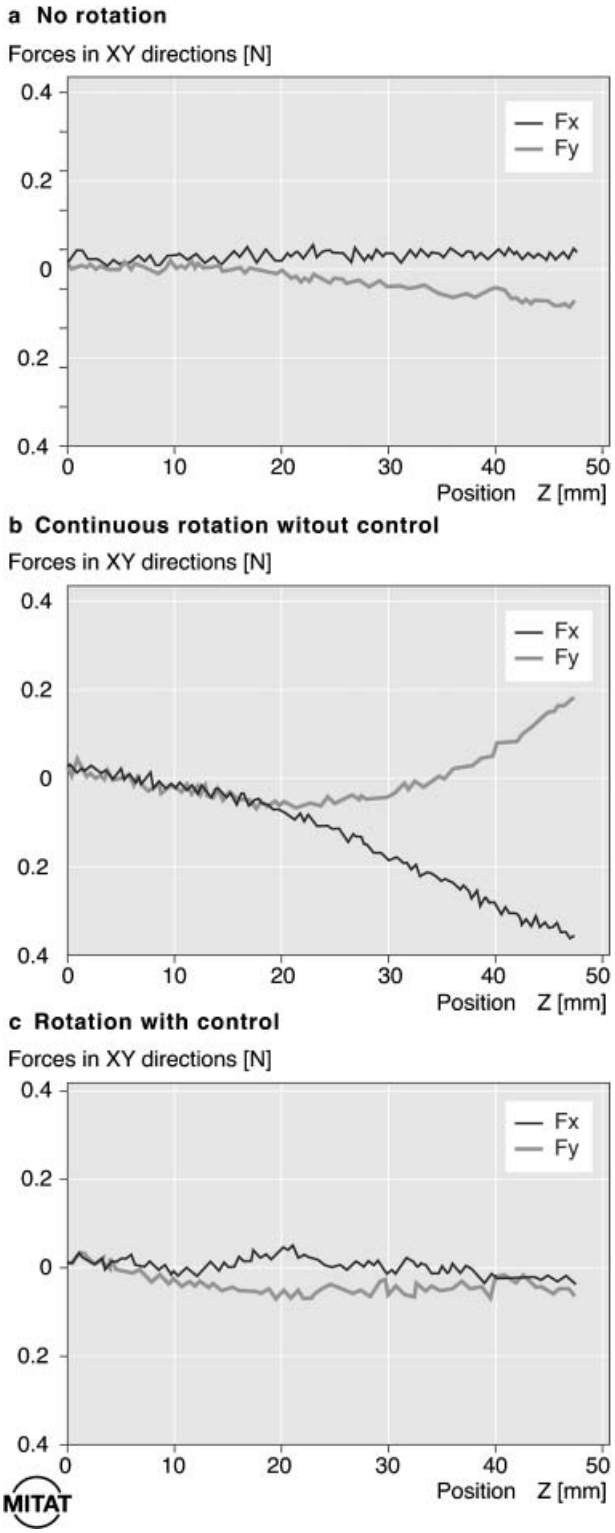

Figure 9. Comparison of the magnitude of the forces in the X–Y plane (a) No rotation (b) Continuous rotation without control (c) Rotation control using X and Y forces.

best approach was to control the rotational motion of the needle by keeping as close to zero as possible the forces orthogonal to the insertion direction. A

trajectory update routine for translational motion was developed which updates the velocity of insertion online according to the desired value of the infinitesimal force per tissue displacement obtained from previous insertions. This was combined with rotational motion to yield a 2-DOF online trajectory generation scheme that gave the best results among all trajectories considered in this research. This study presented methods particularly suitable for situations where multiple needle insertions are to be performed using a robotic system. This study may improve needle insertion in computer-assisted prostate brachytherapy prior to the appearance of the needle tip in the ultrasound field of view.

Acknowledgements

This research was supported by the National Sciences and Engineering Research Council (NSERC) of Canada under Collaborative Health Research Project Grant #262583-2003 and by an infrastructure grant from the Canada Foundation for Innovation.

References

1. Shi M, Liu H, Tao G. A stereo-fluoroscopic image-guided robotic biopsy scheme. IEEE Trans Contr Syst Technol. 2002;10:309–17.
2. DiMaio SP, Salcudean SE. Needle insertion modeling and simulation. IEEE Trans Robot Automat. 2003;19:864–75.
3. Cinquin P, Lavallee S, Troccaz J. Image guided operating robot, methodology and application. Proceedings of the IEEE Conference on Engineering in Medicine and Biology 1993: 1048–9.
4. Alterovitz R, Pouliot J, Taschereau R, et al. Needle insertion and radioactive seed implantation in human tissues. Proceedings of the IEEE Conference on Robotics and Automation 2003 Taiwan, 1793–9.
5. Kataoka H, Washio T, Chinzei K, et al. Measurement of tip and friction acting on a needle during penetration. Proceedings of the Conference on Medical Image Computing and Computer-Assisted Intervention 2002: 216–23.
6. DiMaio SP, Salcudean SE. Needle steering and model-based trajectory planning. Proceedings of the Conference on Medical Image Computing and Computer-Assisted Intervention 2003: 33–40.
7. Nath S, Chen Z, Yue N, Trumpore S, et al. Dosimetric effects of needle divergence in prostate seed implant using 125I and 103Pd radioactive seeds. Med Phys 2000: 1058–66.
8. Pouliot J, Taschereau R, Coté C, Roy J, et al. Dosimetric aspects of Permanents radioactive implants for the treatment of prostate cancer. Physics in Canada. 1999;55:61–8.
9. Okamura AM, Simone C, O'Leary MD. Force modeling for needle insertion into soft tissue. IEEE Trans Biomed Eng. 2004;51:1707–16.
10. DiMaio SP, Salcudean SE. Simulated interactive needle insertion. Proceedings of the 10th IEEE Symposium on Haptic Interfaces for Virtual Environment & Teleoperator Systems 2002: 344–51.
11. Karnopp D. Computer simulation of stick-slip friction in mechanical dynamic systems. Trans. of the ASME, J. of Dynamic Systems, Measurement and Control. 1985; 107:100–3.
12. Maurin B, Barbe L, Bayle B, Zanne P, et al. *In vivo* study of forces during needle insertions. Scientific Workshop on Medical Robotics, Navigation and Visualization (MRNV04); Germany: Remagen, 2004: 415–22.
13. Maurel W. 3D modeling of the human upper limb including the biomechanics of joints muscles and soft tissues. PhD thesis, Laboratoire d'Infographie-Ecole Polytechnique Federale de Lausanne, Switzerland, 1999.
14. Fung YC. Biomechanics - mechanical properties of living tissues. 2nd ed. Springer-Verlag, 1993.
15. Brett PN, Fraser CA, Henniggan M, Griffiths MV, et al. Automatic surgical tools for penetrating flexible tissues. Proceedings of the IEEE Conference on Engineering in Medicine and Biology, 1995: 264–70.
16. Brett PN. Harrison AJ., Thomas TA. Schemes for the identification of tissue types and boundaries at the tool point for surgical needles. IEEE Trans Inform Technol in Biomed. 2000;4:30–6.
17. Matsumiya K, Momoi Y, Kobayashi E, Sugano N, et al. Analysis of forces during robotic needle insertion to human vertebra. Proceedings of the Medical Image Computing and Computer Assisted Intervention Conference; 2003: 271–8.
18. Cotin S. Surgical simulation and training: the state of the art and need for tissue models. IEEE Workshop on Intelligent Robotics and Systems 2003, Las Vegas, 2003.
19. Parker KJ, Huang SR, Musulin RA, Lerner R. M. Tissue response to mechanical vibrations for sonoelasticity imaging. J of Ultrasound in Medicine & Biology. 1990;16:241–6.
20. Brouwer I, Ustin J, Bentley L, Sherman A, et al. Measuring in vivo animal soft tissue properties for haptic modeling in surgical simulation. Proceedings of the Medicine Meets Virtual Reality Conference 2001: 69–74.
21. Han L, Noble JA, Burcher M. A novel ultrasound indentation system for measuring biomechanical properties of *in vivo* soft tissue. J of Ultrasound in Medicine & Biology. 2003; 29:813–23.
22. Menciassi A, Eisinberg A, Carrozza MC, Dario P. Force sensing microinstrument for measuring tissue properties and pulse in microsurgery. IEEE/ ASME Trans on Mechatronics. 2003;8:10–7.
23. Ottensmeyer M, Kerdok AE, Howe RD, Dawson SL. The effects of testing environments on the viscoelastic properties of soft tissues. Proceedings of the Medical Simulation Symposium – ISMS. 2004;3078:9–18.
24. Ottensmeyer MP. TeMPeST 1-D: an instrument for measuring solid organ soft tissue properties. Experimental Techniques. 2002;26:48–50.
25. Céspedes I, Ophir J, Ponnekanti H, Maklad NF. Elastography: Elasticity imaging using ultrasound with application to muscle and breast vivo. Ultrasonic Imaging. 1993;15:73–88.
26. Nava A, Mazzo E, Kleinermann F, Avis NJ, et al. Determination of the mechanical properties of soft human tissues through aspiration experiments. Proceedings of the Medical Image Computing and Computer-Assisted Intervention Conference 2003; Montreal, Canada, 222–9.
27. Brouwer I, Ustin J, Bentley L, Sherman A, et al. Measuring in vivo animal soft tissue properties for haptic modeling in surgical simulation. Proceedings of the Medicine Meets Virtual Reality Conference 2001: 69–74.
28. Brown JD, Rosen J, Kim YS, Chang L, et al. In-vivo an in-situ compressive properties of procine abdominal soft tissues.

Proceedings of the Medicine Meets Virtual Reality Conference 2003: 26–32.
29. Alterovitz R, Pouliot J, Taschereau R, Hsu IJ, et al. Simulating needle insertion and radioactiuve seed implantation for prostate brachytherapy. Proceedings of the Medicine Meets Virtual Reality Conference 2003: 19–25.
30. Kerdok AE, Cotin SM, Ottensmeyer MP, Galea A, et al. Truth cube: Establishing physical standards for real time soft tissue simulation. Bonn, Germany: Workshop on Deformable Modeling and Soft Tissue Simulation, 2001.
31. Howe RD. The truth cube: Establishing standards for soft tissue modeling IEEE Workshop on Intelligent Robotics and Systems, Las Vegas, 2003.
32. Kataoka H, Washio T, Audette M, Mizuhara K. A model for relations between needle deflection, force, and thickness on needle insertion. Proceedings of the Medical Image Computing and Computer-Assisted Intervention Conference 2001: 966–74.
33. Webster III RJ, Memisevic J, Okamura AM. Design considerations for robotic needle steering. Proceedings of the IEEE Conference on Robotics and Automation 2005: 3599–3605.
34. Glozman D, Shoham M. Flexible needle steering and optimal trajectory planning for percutaneous therapies. Proceedings of the Medical Image Computing and Computer-Assisted Intervention Conference; 2004; Saint-Malo, France: 137–44.
35. Webster III RJ, Cowan NJ, Chirikjian G, Okamura AM. Nonholonomic modeling of needle steering. Proceedings of the 9th Symposium on Experimental Robotics, June 2004.
36. Craig JJ. Introduction to Robotics: Mechanics and Control. 2nd ed, Addison-Wesley, Reading, MA, 1989.